Analysis of the on-orbit Response-Versus-Scan-Angle for the MODIS SWIR Bands Derived from Lunar Observations

Truman Wilson[a], Emily Aldoretta[a], Amit Angal[a], Xu Geng[a], Kevin Twedt[a], and Xiaoxiong Xiong[b]

[a]Science Systems and Applications, Inc., 10210 Greenbelt Road, Lanham, MD 20706, USA;
[b]Sciences and Exploration Directorate, NASA/GSFC, Greenbelt, MD 20771, USA

ABSTRACT

The Moderate Resolution Imaging Spectroradiometer (MODIS) on board the Terra and Aqua platforms is a multi-spectral, whiskbroom scanning radiometer with 36 spectral bands covering wavelengths from $0.4 - 14.2$ μm. Among these bands, the 20 reflective solar bands (RSB, $0.4 - 2.1$ μm) use an on-board solar diffuser (SD) and SD stability monitor (SDSM) to track the detector gain changes on orbit. In addition to this, lunar and Earth-view (EV) observations are used in order to characterize the scan-mirror response versus scan angle (RVS), which improves the Earth-view retrieval over the full width of each scan. For the short-wave infrared bands (SWIR, $1.2 - 2.1$ μm), the prelaunch RVS has been used for both Aqua and Terra MODIS throughout each mission. While these bands are not expected to have a significant change in the RVS on-orbit, issues such as electronic crosstalk and an out-of-band optical leak have prevented the use of the Moon for deriving the on-orbit RVS for validation. However, recent improvements to the MODIS lunar calibration for the SWIR bands allow us to mitigate the electronic crosstalk impact and derive the RVS for the SWIR bands. In this work, we will assess the impact of this newly derived RVS on the EV data compared to MODIS Collection 6.1. By comparing to EV data obtained from pseudo-invariant calibration sites at different angles-of-incidence on the scan mirror, we can assess the effectiveness of the newly derived RVS from the Moon. We find that while the change in the RVS on-orbit for the SWIR bands is relatively small, applying a correction to the RVS based on the Moon and SD data can provide an improvement for some bands.

Keywords: MODIS, Calibration, short-wave infrared, response versus scan angle, lunar calibration, crosstalk

1. INTRODUCTION

The Moderate Resolution Imaging Spectroradiometer (MODIS) has been in operation on the Terra and Aqua platforms since 2000 and 2002, respectively.[1] MODIS is a whisk-broom scanning radiometer, with 36 spectral bands that range from the visible (VIS) to the long-wave infrared (LWIR) wavelength range. Among these spectral bands are 20 reflective solar bands (RSB) with wavelengths ranging from $0.4 - 2.1$ μm and 16 thermal emissive bands (TEB) with wavelengths ranging from $3.6 - 14.2$ μm. MODIS collects Earth-view (EV) imagery at 3 spatial resolutions at nadir, with bands $1 - 2$ at 250 m (40 detectors/band), bands $3 - 7$ at 500 m (20 detectors/band), and bands $8 - 36$ at 1 km (10 detectors/band). The bands are separated by wavelength onto 4 separate focal plane assemblies (FPA) for the VIS, near-infrared (NIR), short-wave and mid-wave infrared (S/MWIR), and LWIR. For each MODIS scan, an image of the Earth is acquired that is 10 km wide in the track direction at nadir and 2,330 km wide in the scan direction. The MODIS scan-mirror is double sided and alternates views of the Earth between each scan. Each scan spans an angular field-of-view (FOV) that is $\pm 55°$ from nadir, and ranges between $10.5°$ and $60.5°$ in angle of incidence (AOI) on the scan mirror. During a scan, the data sampling for each detector is divided into 1354 frames each with an equal angular FOV. For the 250-m and 500-m bands, 4 and 2 additional subframes are added per frame in order maintain an equal resolution in the scan and track directions at nadir, respectively. A diagram of the MODIS instrument and scan mirror AOIs can be seen in Figure 1.

Further author information: (Send correspondence to T.W.)
T.W.: E-mail: truman.wilson@ssaihq.com, Telephone: 1 301 867 2120

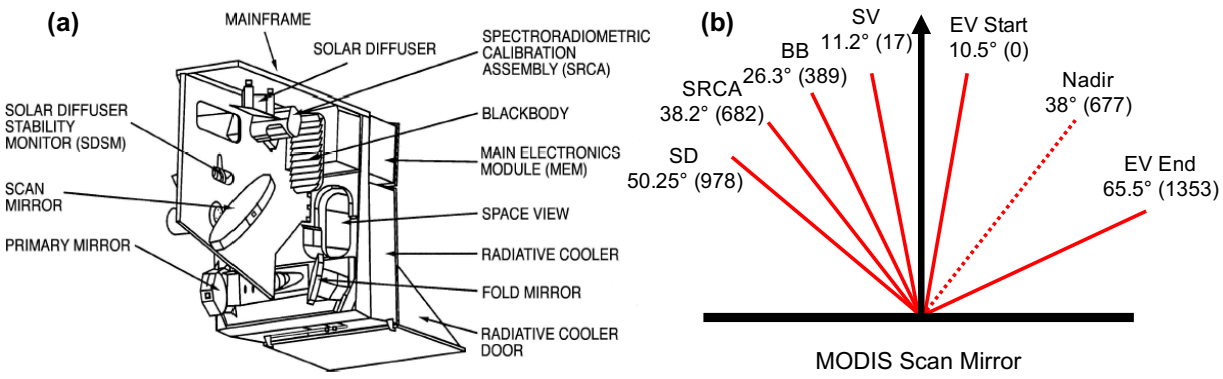

Figure 1. (a) A diagram of the MODIS instrument. (b) A diagram of the scan-mirror AOIs for the onboard calibrators and EV sectors. The angle of incidence is listed along with its corresponding frame number in the EV data sector in parentheses.

To ensure the retrieval of climate quality data throughout each mission, the MODIS bands are calibrated on-orbit using a set of onboard calibrators. A solar diffuser (SD) and its associated SD stability monitor (SDSM) are used to calibrate the RSB. The SD calibration is typically operated in two modes, one of which occurs with the sunlight restricted by a pinhole screen which allows the calibration of the high-gain ocean color bands, and the other with the screen removed. However, for Terra MODIS, the SD calibration has taken place with the pinhole screen in place since July 2003 due to an anomaly with the motor that controls the SD door and pinhole screen. In addition to the SD calibration, MODIS views the Moon through the space-view (SV) port using regularly-scheduled lunar roll maneuvers.[2,3] These maneuvers allow observations of the Moon in a narrow phase angle range, providing consistency between observations. Since the Moon can be considered a stable reflectance source, and because it occurs at a different AOI on the MODIS scan mirror compared to the SD, monitoring the trends from the SD and Moon allow for the characterization of the scan-mirror response versus scan angle (RVS). In recent years, additional data from EV observations of pseudo-invariant calibration sites (PICS) have been used to enhance the RVS characterization of select short-wavelength bands.[4]

For the MODIS SWIR bands, signal contamination in the form of both electronic crosstalk and an out-of-band optical leak at 5.3 µm have impacted the data at all levels throughout the entirety of both missions. The impact has been particularly severe for Terra MODIS, which has resulted in very large sub-sample differences in the Level-1B (L1B) data.[5,6] These effects have been studied extensively, and a correction to the SWIR data has been applied since Collection 2 with a recent update for Terra MODIS in Collection 6.1.[7] The SWIR correction uses a special Night-time Day-mode (NTDM) data collection, since the RSB data is not nominally sent down from the spacecraft during night mode.[5] The data size during night mode is significantly reduced with no reduction in usable data from the instrument since there is no reflected solar signal measured by the RSB. During this data collection, any signal measured by the SWIR bands is expected to be caused by contamination from either the optical leak or electronic crosstalk from the TEB. Since MODIS does not have a band at 5.3 µm, the TEB with the best signal correlation is used to provide a correction. It was found that bands 28 (7.3 µm) and 25 (4.5 µm) showed the best correlation early in the mission for Terra and Aqua MODIS, respectively. However, the increased presence of electronic crosstalk in Terra MODIS band 28 after the 2016 safe mode event has led to the switch to band 25 as a reference band in the latest collection.[7]

For the lunar data, a contamination correction using band 25 (or any TEB) is not possible since the Moon signal is saturated for most of the pixels. For this reason, the lunar data has not been used in the RVS characterization for the MODIS SWIR bands, and the pre-launch RVS has been used throughout the mission. While the RVS has not been updated on orbit for the SWIR bands, the EV products have not shown any significant evidence of a scan-angle dependence for these bands. Also, for RSB in the SWIR wavelength range, the surface degradation of both the scan mirror and SD is expected to be relatively small compared to the other RSB.[8] However, it is necessary to have an independent validation of the SWIR RVS and to have the proper

methodology in place in case a change does take place on orbit. In recent investigations, a correction for both the electronic crosstalk and optical leak contamination was derived using lunar observations in an effort to reduce the subsample difference in Terra MODIS.[6] In the Moon images, the electronic component is clearly separated from the main image due to the spatial offsets of the sending bands on the FPA. By removing this contamination, the oscillations in the lunar trend were greatly reduced. This will allow us to derive the trending gain throughout the mission from the lunar data, which we can then use along with the SD data to evaluate the RVS change on-orbit for the SWIR bands.

In this work, we will apply a data masking algorithm to the lunar data in order to remove the impact of electronic crosstalk from the lunar calibration data. Using this lunar data in combination with the SD data trend, we will calculate the RVS for the SWIR bands and compare the change throughout the mission to the pre-launch (PL) values. In Section 2, we will discuss the Moon and SD calibration approach. We will review the specifics of both the SD and lunar calibration algorithms, and show our improvements to the lunar gain trending using our data masking approach. In Section 3, we will then compute the RVS as a function of time based on the differences between these two trends by applying a linear correction based on the SD and lunar data to the PL RVS data. We then assess the changes to the RVS compared to the PL data over time for both instruments. In Section 4, we can assess the impact of the RVS change from the Moon and SD-based approach on EV scenes by analyzing the reflectance trending from select PICS. Finally, in Section 5, we will present our conclusions.

2. MODIS SD AND LUNAR CALIBRATION

To compute the RVS for the MODIS RSB, the MODIS Characterization Support Team (MCST) developed an algorithm that tracks gain degradation as measured from the SD and Moon data, which are located at two different AOIs on the MODIS scan mirror.[4] The MODIS RSB calibration algorithm has been covered extensively in previous work.[2,4,9] Therefore, we will only review the SD and Lunar calibration algorithms briefly below. The EV data in the case of SWIR bands is not expected to provide any enhancement if a reliable lunar trend is available. Therefore, we will skip this discussion here and focus on only the parts of the calibration relevant to the SWIR bands. However, the EV data will provide a useful assessment of the impact of the correction and will be shown in Section 4.

2.1 Solar Diffuser Calibration

The primary target for the on-board calibration of the MODIS RSB is the SD with its associated SDSM. The MODIS SD is comprised of a Spectralon panel which provides a diffuse solar reflection that is directed towards the MODIS bands through the main optical path. The SDSM is located near the SD and is used to monitor the degradation of the SD surface reflectance by alternating views of direct sunlight and the SD reflected light. The SD calibration typically operates in two modes, one with an open port view of the Sun and another with a pinhole screen in place to limit the sunlight that illuminates the SD. The calibrations with the pinhole screen are used for the high-gain ocean color bands. While both of these modes are currently in use for Aqua MODIS, for Terra, a mechanical anomaly required the pinhole screen to remain in place since July 2003. Therefore, all of the Terra RSB since that time are calibrated using data with the pinhole screen in place. An additional scaling ratio is applied to the calibration coefficients at the point of transition in order to ensure that the data is continuous across this boundary.

The MODIS SD calibration algorithm is covered in detail in many previous works.[9] The goal of the SD calibration is to compute the calibration coefficient, m_1, which can be calculated from the following equation:

$$m_1 = \frac{\rho_{\mathrm{SD}} \cos\left(\theta_{\mathrm{SD}}\right)}{dn^* \cdot d_{\mathrm{ES}}^2} \cdot \Gamma_{\mathrm{SDS}} \cdot \Delta_{\mathrm{SD}} \tag{1}$$

where ρ_{SD} is the PL bi-directional reflectance factor (BRF) of the SD, θ_{SD} is the solar zenith angle on the SD, Γ_{SDS} is the pinhole screen vignetting function (equal to 1 when the screen is open), Δ_{SD} is the SD degradation factor derived from the SDSM, dn^* is the background-subtracted, temperature-corrected SD signal level, and d_{ES} is the Earth-Sun distance. The m_1 values are computed on the detector, mirror-side, and subframe level for each band. For the MODIS SWIR bands, an additional correction is applied to the dn^* term associated with

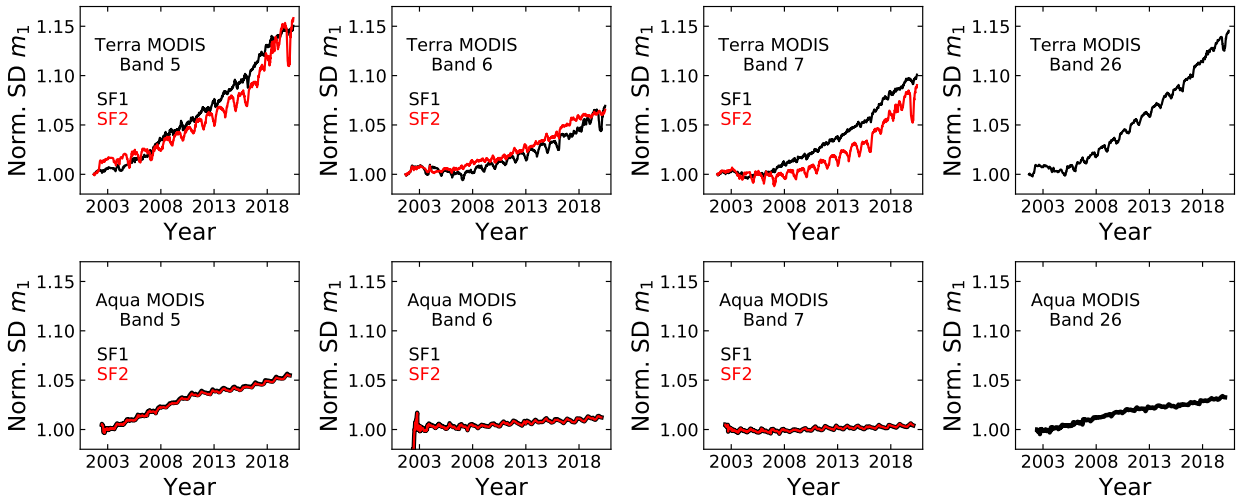

Figure 2. Trending of the normalized SD m_1 values for Terra and Aqua MODIS for subframe 1 (black) and subframe 2 (red). The data here is shown for mirror-side 1. The data for band 26 only has one subframe.

the electronic crosstalk and optical leak correction. In the current MODIS data, band 25 is used as a reference band for this correction and is applied using a linear equation for each detector and subframe as follows:

$$dn^*_{\text{cor}} = dn^*_{\text{unc}} - c \cdot dn_{\text{ref}} \tag{2}$$

where c is the correction coefficient for the corresponding detector, subframe, and mirror-side and dn_{ref} is the background-subtracted signal for band 25. This correction is also applied to the EV data. The correction coefficients are derived from NTDM data, where data collected from EV scenes at night for the SWIR bands are only expected to have signal contribution from contamination. While both Aqua and Terra use band 25 as a reference band for the contamination in the current collection, for Terra, band 28 was used historically, before July 2019. Early in the mission, band 28 was found to have the highest correlation with the contaminated signal. However, the increasing impact of electronic crosstalk in Terra MODIS bands $27-30$ after the 2016 safe mode event led to secondary effects in the Terra SWIR bands that necessitated the switch to band 25.

For Terra MODIS, the instrument electronics side and data formatter side were changed multiple times during the early part of the mission. As a result, the gain of the SWIR bands in particular changed multiple times from launch up to September 2001, after which the gain trends more smoothly. During this time, the lunar data which is used in conjunction with the SD data has very few points at any given electronics setting. Therefore, a long-term trend used to determine the RVS is not easily derived. For this work, we will consider the trending in both the SD data here and the lunar data in Section 2.2 from September 2001 onward, assuming that the RVS change before this time is relatively small.

The SD trending data for both instruments can be seen in Figure 2. The m_1 data shown in this figure is for mirror-side 1, with similar trends existing for mirror-side 2. For Terra MODIS, the electronic crosstalk/optical leak contamination causes a larger difference in the subframe-dependent m_1 values when compared to Aqua, even with a correction applied. For the subframe with the larger contribution from electronic crosstalk (subframe 2 for bands 5 and 7 and subframe 1 for band 6), we see larger amplitude oscillations in the m_1 values. However, when deriving the RVS in Section 3, we will use piecewise fitting of the m_1 trends in order to remove the impact from these oscillations.

2.2 Lunar Calibration

Throughout each mission, both MODIS instruments have used regularly-scheduled spacecraft roll maneuvers in order to observe the Moon on a near-monthly basis.[3] These observations have been used for tracking radiometric

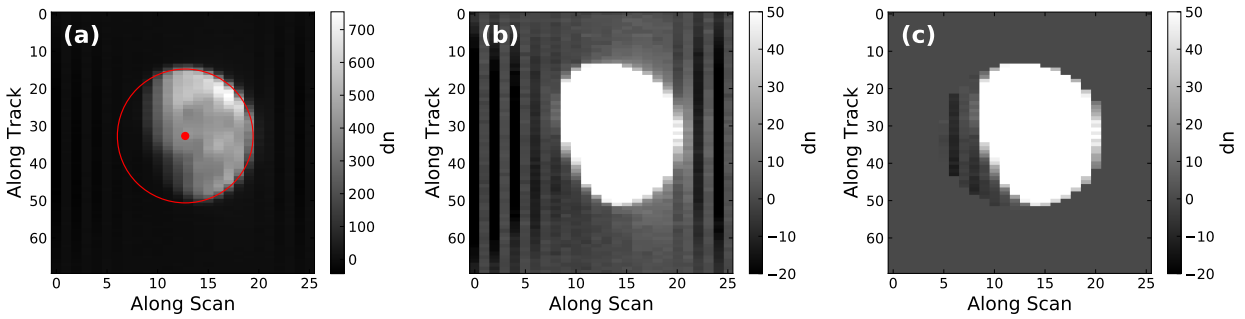

Figure 3. Data masking example for Terra MODIS Band 6 from January 14, 2020. (a) Full scale image (from a single detector) with the elliptical fit shown in red. The Moon's center is indicated by the red dot. (b) Truncated scale image to show the contamination outside the main lunar signal. (c) Truncated image with data mask applied.

gain changes of the RSB in order to characterize the scan mirror RVS, spatial registration assessments, and the correction of electronic crosstalk.[2,10,11] As of August 1, 2020, 201 and 189 scheduled lunar observations are used in Terra and Aqua MODIS RVS calculation, respectively. The details of the MODIS lunar calibration algorithm can be found in Reference 2 and will be reviewed briefly here.

While the scan mirror rotation rate is set such that the EV images at nadir can be stitched together to create a continuous image, the much greater distance to the Moon results in the Moon being visible for many successive scans through the SV port. As a consequence, the Moon is oversampled by the MODIS detectors, and will shift less than the width of a single 1-km MODIS pixel from scan to scan. We can take advantage of this oversampling to create images of the Moon for each detector, which are created by combining data from multiple scans into a single image. An example of this detector-level imagery can be seen in Figure 3(a). The lunar m_1 values can be found by taking the inverse of the measured gain, G, derived from the lunar data. The gain is given by:

$$G = \frac{1}{N_{\mathrm{D}} \cdot f_{\mathrm{n}} \cdot f_{\mathrm{os}}} \sum_{I_{\mathrm{D}}} m_1^{\mathrm{pl}} \cdot dn^* \tag{3}$$

where m_1^{pl} are the PL m_1 values at the detector, subframe, and mirror-side level, and dn^* is the temperature-corrected background-subtracted digital signal. These terms are summed over each detector-level image (I_{D}) and then divided by the number of operable detectors in the band, N_{D} (dn is set to zero for inoperable detectors). The geometry normalization factor f_{n} is used to correct for lunar observations differences, such as the Sun-Moon and Moon-instrument distance, lunar phase angle and the lunar libration angles. These geometric normalization parameters are derived from the USGS ROLO model.[12] The f_{os} term is an oversampling factor correction.

For the SWIR bands, both an out-of-band optical leak and electronic crosstalk have impacted the data since the early part of each mission.[5] These effects have negatively impacted the lunar data, particularly for Terra MODIS.[6] However, since the RVS for the SWIR bands is expected to be small compared to the other RSB, the lunar calibration results have not been applied in the calibration algorithm, and the PL RVS results have been used for all of the SWIR bands in both instruments. For the SD and EV data, the band 25 reference signal is used to correct the SWIR band data. However, the lunar data presents some difficulties for this approach. First, the signal for all of the TEB including band 25 is, in general, much higher than that of the RSB when viewing the Moon. In fact, for band 25, the signal saturates for most of the lunar pixels. Therefore, applying the band 25 correction in the same way as the SD and EV data significantly reduces the quality of the lunar data. Second, the spatial offsets of the electronic component of the contamination play a more significant role in the lunar data given the small size of the Moon image on the FPA. In this case, most of the electronic contamination is seen away from the main lunar image in the background, as shown in Figure 3. In recent years, methods have been developed for correcting the electronic component of the contamination in the lunar data that are based on the same principles as the implementation to the PV LWIR bands ($27-30$) in Terra MODIS Collection 6.1.[13] This methodology involves accounting for the contamination sent by several bands, many of which saturate when

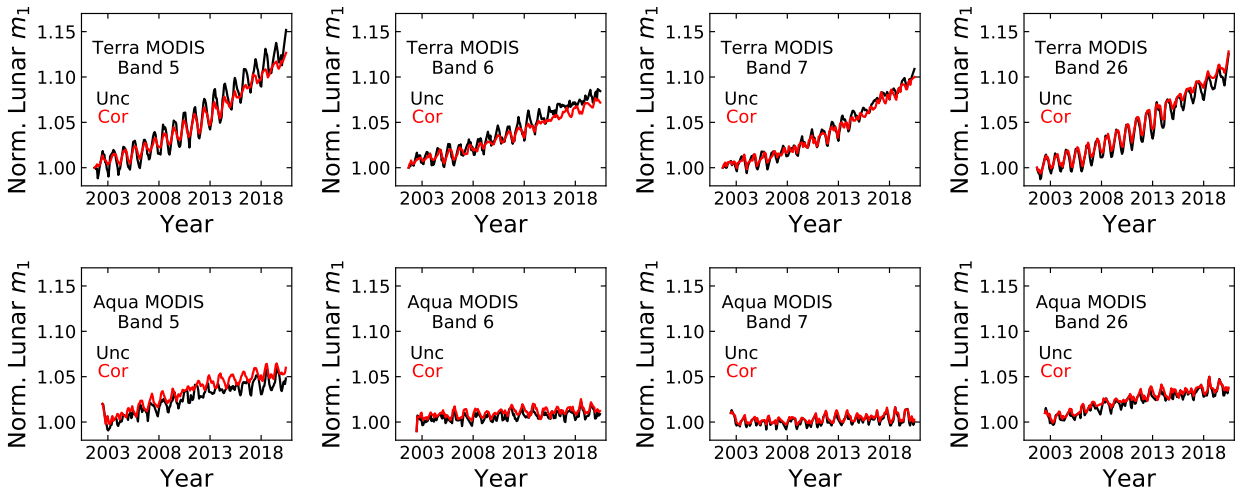

Figure 4. Trending of the normalized lunar m_1 values for Terra and Aqua MODIS without (black) and with (red) a data mask applied.

viewing the Moon, and finding the correction coefficients by correlating the contaminated and sending signal using the appropriate sample timing offsets. For our work, we do not need to derive correction coefficients from the lunar data, as those from band 25 will be applied to the SD and EV data. Therefore, in order to simplify the approach, we adopt a simple data masking scheme to remove the electronic contamination from the lunar data away from the main lunar signal.

The data masking approach is simple and is shown in Figure 3. First, we take a detector-level image of the Moon and apply a Sobel filter in order to determine the location of the Moon limb. We then fit a ellipse to the Moon limb with the aspect ratio set to be the oversampling factor. An example of this elliptical fitting can be seen in Figure 3(a). In Figure 3(b), we truncate the scale of the Moon image in order to highlight the contamination that exists away from the main lunar signal. In Figure 3(c), we use a 1.5 pixel buffer to our elliptical fit to apply a mask to the data, with any pixel with a center location outside of our mask set to zero. We can see here that the majority of the electronic contamination can be removed without the need for accounting for the individual sending signals.

A comparison of the masked data to the non-masked data can be seen in Figure 4. The main effect of the masking is a reduction in the oscillations in the data, particularly for Terra MODIS. However, a slight difference in the trend can be observed for some of the bands. This impact is expected, as previous work has shown that the level of contamination from both the electronic and optical components has been relatively stable throughout the mission.[5,6] The remaining oscillations in the data are associated with the lunar librations residuals from the geometric model correction.[12] These oscillations are a well known phenomenon and are common to all of the MODIS bands.

The data masking can also be applied to improve the mirror-side ratio calculation, which is used to help determine the RVS difference between the two mirror sides. The mirror-side ratio calculation is simple. We first first remove data from inoperable detectors (for Aqua band 6 in particular) and then take the sum of the signals measured by each mirror-side and divide them together. The results of this calculation can be seen in Figure 5. For lunar data, each mirror-side does not necessarily see the exact same area of the Moon as it traverses the FPA during the observation. Therefore, the lunar mirror-side ratio tends to show more outliers when compared to the lunar m_1 data. However, in the case of the SWIR bands, the long-term trend can be easily determined and shows less than a 0.5% change throughout the mission for each band. We'll note that since Aqua band 6 has fewer operable detectors, the magnitude of the outlier data is increased compared to the other bands. However, the long-term trend for this band is still stable.

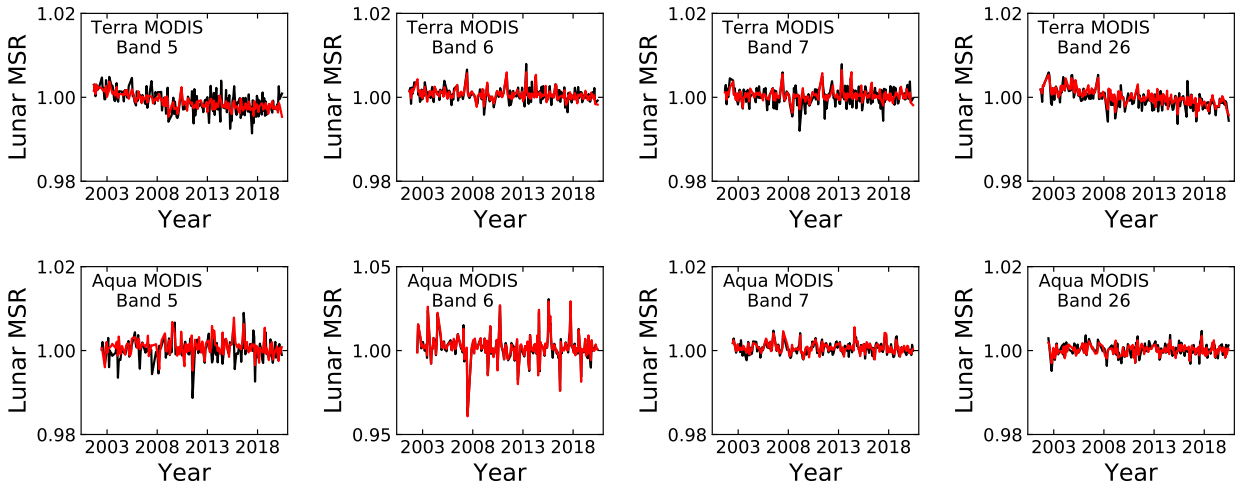

Figure 5. Trending mirror-side ratio for Terra and Aqua MODIS without (black) and with (red) a data mask applied. The scale is increased for Aqua band 6 since the lack of operable detectors causes more noise in the data.

3. DERIVING THE RVS FROM SD AND LUNAR DATA

With the trending data from both the SD and the Moon, we can derive the change in the on-orbit RVS using a simple linear scaling approach applied to the PL RVS. The PL RVS was characterized using an integrating sphere at 13 different AOIs, and is assumed to not have any significant changes between the time of this characterization and the instrument launch.[14] Examples of the PL RVS values for band 7 of each instrument can be seen in Figure 6. To measure the changes in the RVS, we look at the difference in trending of the normalized m_1 values at the AOI of the SD (50.25°, frame 978) and the SV (11.2°, frame 17) (see Figure 1(b)). The trends shown in Figure 2 and Figure 4 are fit with a piece-wise polynomial function in order to remove the seasonal oscillations from the data. The difference in the m_1 trending since the start of the mission (or September 2001 in the case of Terra) is assumed to be linear over AOI (or frame number) and the change per degree can be computed from the two points at the SD and SV AOI. This linear change is then multiplied by the PL RVS and normalized to the value at the SD. Examples of the RVS for band 7 in Terra and Aqua over several years are shown in Figure 6. We can note the scale change between Terra and Aqua, which shows that Terra had a larger range in the RVS during PL and also shows a larger change on-orbit.

To better understand the nature of the RVS change, we can also look at the time series of the change compared to the PL data at select frames, as seen in Figure 7. Here we look at four frames that span close to the full range

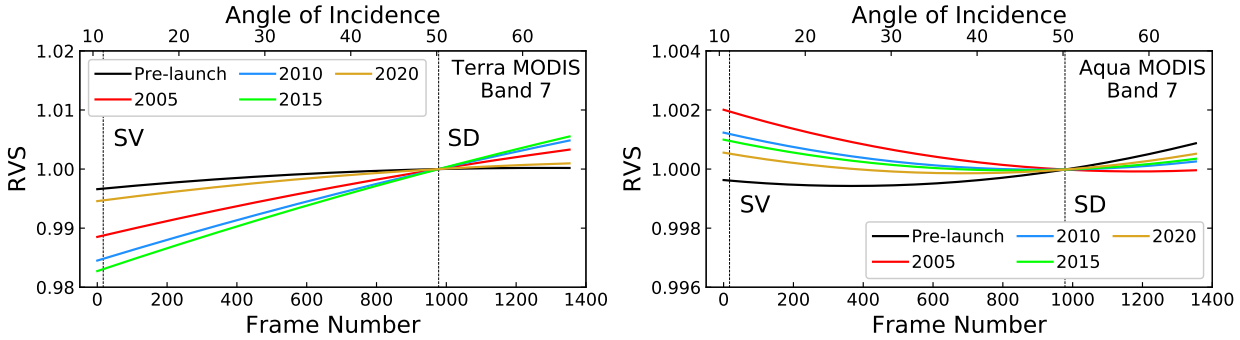

Figure 6. RVS as a function of frame number (AOI shown at top) for Terra and Aqua MODIS band 7. The data shown here is for mirror-side 1, with similar trends existing for mirror-side 2.

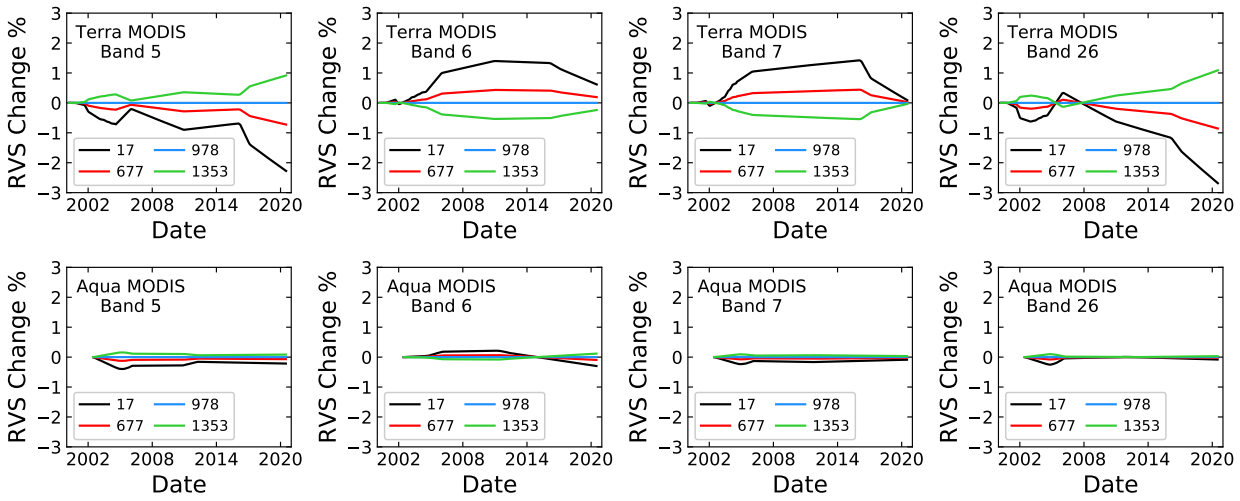

Figure 7. RVS change compared to PL data as a function of time for select frame numbers. Frame 978 is the SD frame and shows no change by definition. The data here is shown for mirror-side 1, with similar changes seen for mirror-side 2.

of AOI. It can be seen clearly here that Aqua MODIS shows the smallest change across all of the bands, with less than 0.5% change for all of the bands across the full range of AOI. For Terra, the change is more pronounced, with an approximately 3% change at the SV frame for band 26. For Terra, we also see a sharp change in the RVS at the February 2016 safe-mode anomaly. Here we see increases in the RVS differences for bands 5 and 26 and decreases for bands 6 and 7. When looking at the SD and lunar m_1 trends, the change in the data at the safe-mode boundary appears more clearly in the SD data compared to the Moon data, where no change in the trend can be observed. This may be related to the application of the crosstalk and optical leak correction to the SD, which is not applied to the lunar data in the same manner, as discussed in Section 2.2. Since the SD m_1 data is calculated for Terra MODIS with the pinhole screen fixed in place, the signal size of the SWIR band calibration is very low compared to that of the band 25 reference band for the contamination. Because of this, it may be more sensitive to the small changes that occurred at the safe-mode boundary to band 25 than it would be with the screen open. However, although these changes are large when compared to Aqua MODIS, they are much smaller than the changes seen over the mission for other bands in Terra MODIS. For Terra MODIS band 8, the change can be greater than 30% at the SV, compared to less than 3% for the SWIR bands shown here.

4. COMPARISON TO DESERT TRENDING

While the changes to the RVS derived from the Moon data are expected to be relatively small, we can use PICS to assess the impact of applying the correction to the MODIS data and compare the results to the PL RVS values. For both MODIS instruments, the satellite ground track repeats in a 16-day cycle allowing us to measure the reflectance of the same target at multiple AOIs on the scan mirror throughout the entire mission. The sampled AOI will span across nearly the full range of AOI through the EV port. The PICS that we will use in this work will come from the Libyan desert. In particular, Figures 8 and 9 will show data from Libya 1 (24.42° N, 13.35° E), with the other sites showing similar trends. We choose 4 AOI to analyze that are close in frame number to those shown in Figure 7, which span over nearly the full range of the EV AOI. For each overpass at the specified frame, a 40 sample (scan) by 20 sample (track) area is integrated to produce the trending signal. Data from bands 1 and 2 are used for cloud screening, and if the standard deviation of either band is greater than 5% of the signal level, the data from that date is rejected. An empirical correction for the surface BRF accounting for the solar angle and view angle geometry is applied to the integrated signal at each AOI in order to reduce the seasonal oscillations in the data.[15] These oscillations are on the order of a few percent for the SWIR bands and are greater near the edge of scan compared to nadir. The data is then normalized for each AOI at the first data point so that the trends show us the change in the RVS over time. The data over desert sites for the SWIR bands is somewhat noisy, so we use quadratic fits to better highlight the trend of the data over the full mission.

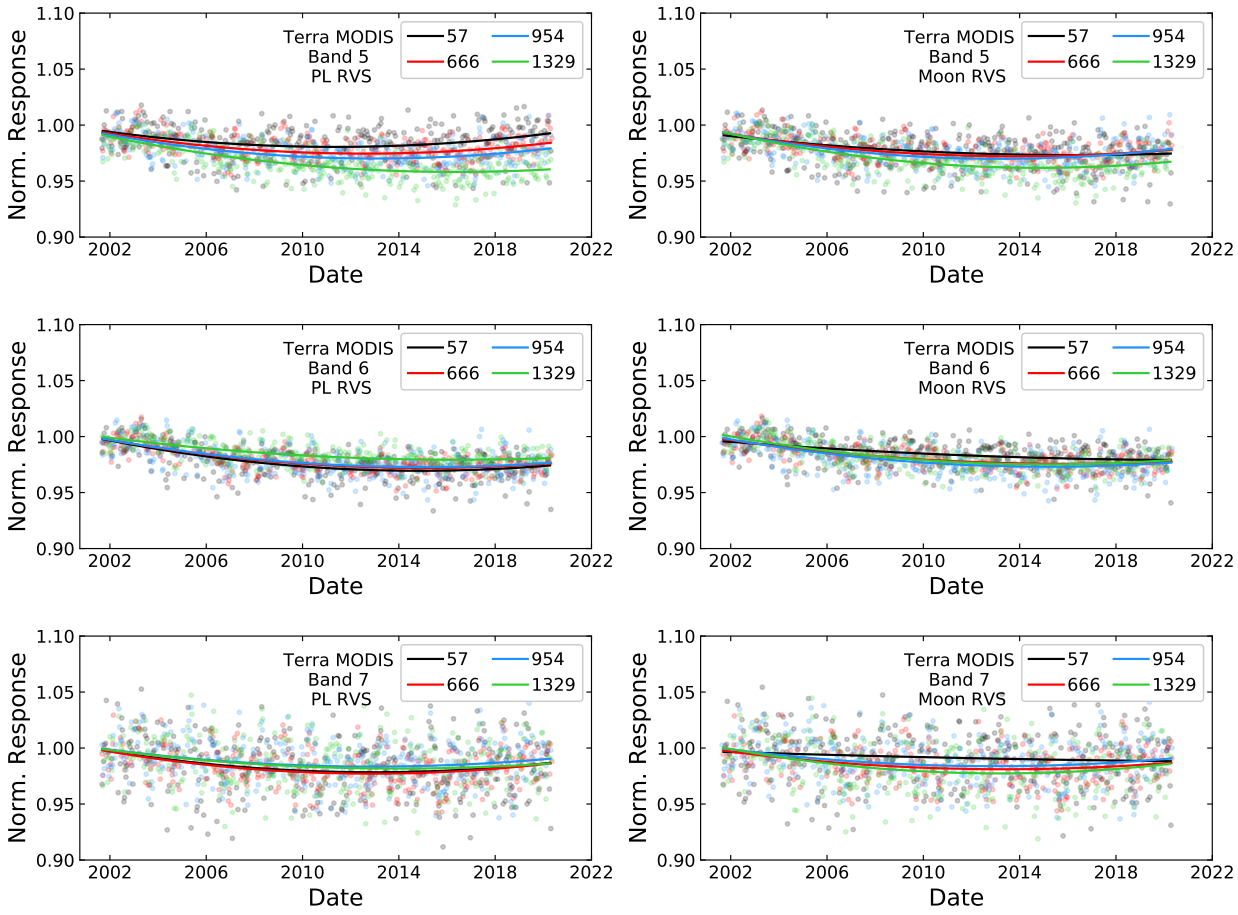

Figure 8. Desert trending results for Terra MODIS bands $5-7$ at frames 57 (black), 666 (red), 954 (blue), and 1329 (green). The left column shows the results using the PL RVS and the right column shows the results of the Moon-based RVS. The symbols show the raw data at each AOI with the lines representing quadratic fits. The symbols are slightly faded so that the lines can be seen more easily.

Also, for the SWIR bands, only bands $5-7$ retrieve a good signal over desert sites. For band 26, the signal level is relatively low and noisy and typically only has high signal over cloudy scenes.

In Figure 8, we show the results for Terra MODIS bands $5-7$. For the PL RVS results, band 5 shows the most change across AOI among the bands. After applying the Moon-based RVS results, we can see that the difference in the trends are reduced from about 4% to around 2% over the full range of AOI. For bands 6 and 7, the change is small compared to band 5, with some changes in the edge frame data over the course of the mission. However, the total difference remains small for these two bands. The small spread in the desert trends of the AOI for all of these bands show that the PL RVS performs reasonably well, but also shows that a Moon-based RVS is able to improve the results slightly, particularly for band 5. Both before and after the correction, we do notice that there is a small drift in the data for each band on the order of $1-2\%$. Since the RVS only changes the gain across all AOI relative to the SD, the application of the RVS will not be able to remove this overall trend in the data, and is therefore being addressed separately.

For Aqua MODIS, the change in the RVS was expected to be very small based on the results shown in Figure 7. The desert results shown in Figure 9 are in good agreement with these expectations. For each band, the spread in the trends across AOI is less than 2% both before and after the Moon-based RVS is applied. This result indicates that the PL RVS is still performing well on orbit.

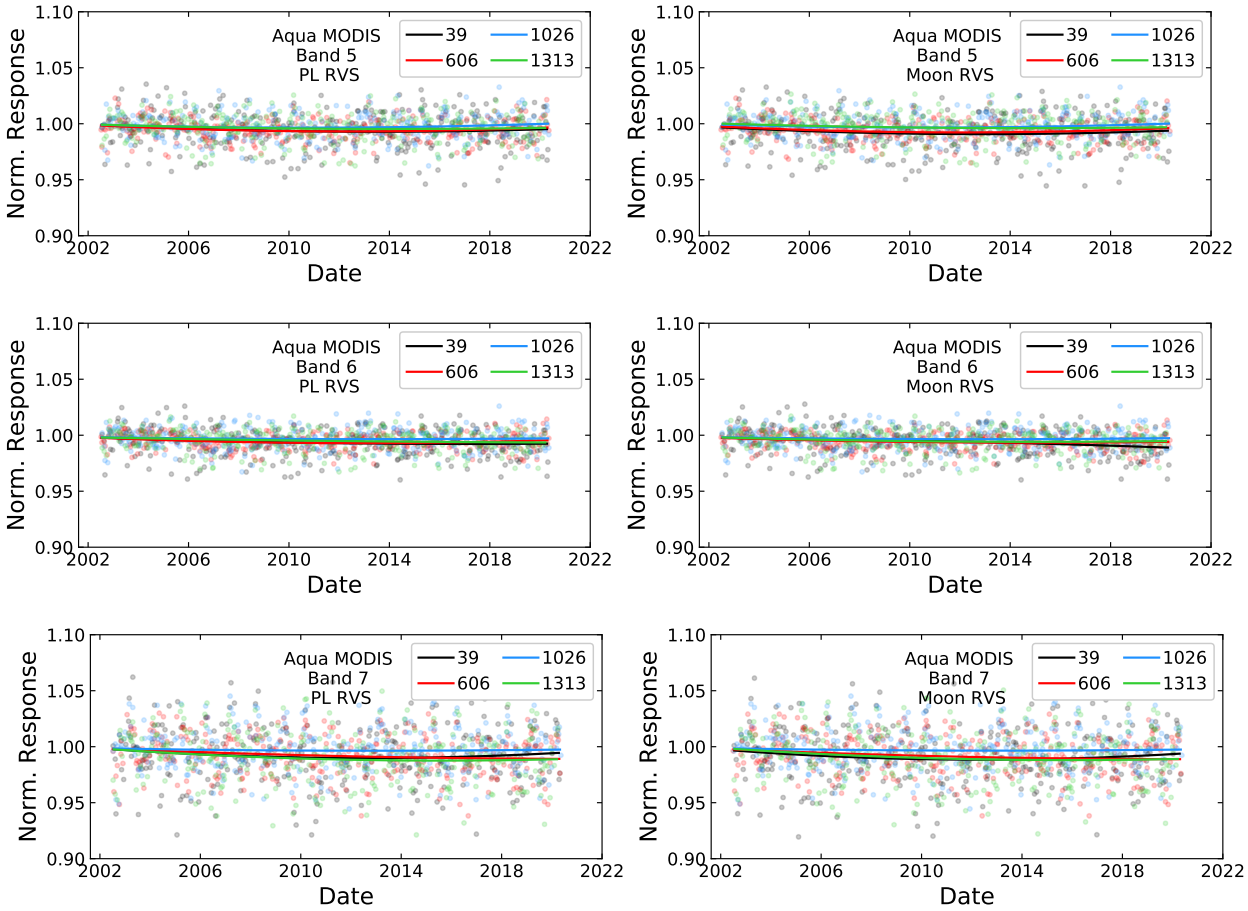

d

Figure 9. Desert trending results for Aqua MODIS bands $5-7$ at frames 39 (black), 606 (red), 1026 (blue), and 1313 (green). The left column shows the results using the PL RVS and the right column shows the results of the Moon-based RVS. The symbols show the raw data at each AOI with the lines representing quadratic fits. The symbols are slightly faded so that the lines can be seen more easily.

5. CONCLUSIONS

In this work, we derived the on-orbit RVS for the MODIS SWIR bands using observations of the Moon and SD. For the Moon data, a masking approach was used to remove the effects of electronic crosstalk, which resulted in a reduction of the oscillations in the lunar calibration coefficient trend. The Moon data and SD data trends were then used to apply a two-point correction to the PL RVS data in order to show the expected change in the RVS over time. For Terra MODIS, the changes were shown to be larger than what is seen in Aqua MODIS, with differences in Terra bands 5 and 26 that could be greater than 3% in 2020 compared to early in the mission. This may be due to the higher magnitude of electronic crosstalk and optical leak contamination that is present in the Terra data, which may impact both the SD and lunar calibrations. Finally, we assessed the impact of the new RVS by applying it to the trending results over desert PICS. These results showed that while the change in the RVS over the mission is small in comparison to other MODIS bands, the new Moon-based RVS might offer some improvement to the results across the full range of AOI, particularly for Terra band 5. For this band, the spread in the RVS over the mission was reduced from 4% to less than 2% over the course of the mission. For Aqua MODIS, the spread in the RVS was less than 2% both before and after the application of the Moon and SD based RVS, with little difference between the two datasets as expected. Overall, the PL RVS still performs well, particularly for Aqua MODIS.

ACKNOWLEDGMENTS

The authors would like to thank all of the current and former members of the MODIS Characterization Support Team (MCST) for all of their valuable contributions to the full history of this work. Work on the MODIS RSB RVS has been on-going for many years and has shown many challenges which have been continually met by various members of MCST throughout the years. We would also like to thank Tiejun Chang for his review of this work.

REFERENCES

[1] Salomonson, V. V., Barnes, W. L., Xiong, X., Kempler, S., and Masuoka, E., "An overview of Earth Observing System MODIS instrument and associated data systems performance," *Proc. IGARSS* **2**, 1174–1176 (2002).

[2] Sun, J., Xiong, X., Barnes, W., and Guenther, B., "MODIS reflective solar bands on-orbit lunar calibration," *IEEE Trans. Geosci. Rem. Sens.* **45**(7), 2383 (2007).

[3] Wilson, T. and Xiong, X., "Planning lunar observations for satellite missions in low-earth orbit," *J. Appl. Remote Sens.* **13**(2), 024513 (2019).

[4] Sun, J., Xiong, X., Angal, A., Chen, H., Wu, A., and Geng, X., "Time-dependent response versus scan angle for MODIS reflective solar bands," *IEEE Trans. Geosci. Rem. Sens.* **52**(6), 3159–3174 (2014).

[5] Xiong, X., Chiang, K., Adimi, F., Li, W., Yatagai, H., and Barnes, W., "MODIS correction algorithm for out-of-band response in the short-wave IR bands," *Proc. SPIE* **5234**, 605–613 (2004).

[6] Wilson, T. and Xiong, X., "Subsample difference correction for terra MODIS SWIR bands 5-7 using lunar observations," *Proc. SPIE* **10785**, 107851B (2018).

[7] Xiong, X., Angal, A., and Li, Y., "Improvements in the on-orbit calibration of the Terra MODIS short-wave infrared spectral bands," *Proc. SPIE* **10781**, 107811C (2018).

[8] Twedt, K. A., Angal, A., Xiong, X., Geng, X., and Chen, H., "MODIS solar diffuser degradation at short-wave infrared band wavelengths," *Proc. SPIE* **10402**, 104022K (2017).

[9] Xiong, X., Chiang, K., Esposito, J., Guenther, B., and Barnes, W. L., "MODIS on-orbit calibration and characterization," *Metrologia* **40**, 89–92 (2003).

[10] Xiong, X., Sun, J., Xiong, S., and Barnes, W. L., "Using the Moon for MODIS on-orbit spatial characterization," *Proc. SPIE* **5234**, 480 (2004).

[11] Sun, J., Xiong, X., Madhavan, S., and Wenny, B. N., "Terra MODIS band 27 electronic crosstalk effect and its removal," *IEEE Trans. Geosci. Remote Sens.* **52**(3), 1551 (2014).

[12] Kieffer, H. H. and Stone, T. C., "The spectral irradiance of the Moon," *Astron. J.* **129**(6), 2887–2901 (2005).

[13] Wilson, T., Wu, A., Shrestha, A., Geng, X., Wang, Z., Moeller, C., Frey, R., and Xiong, X., "Development and implementation of an electronic crosstalk correction for bands 27-30 in Terra MODIS collection 6," *Remote Sens.* **9**(6), 569 (2017).

[14] Barnes, W., Pagano, T., and Salomonson, V., "Prelaunch characteristics of the Moderate Resolution Imaging Spectroradiometer (MODIS) on EOS-AM1," *IEEE Trans. Geosci. Rem. Sens.* **36**(4), 1088–1100 (1998).

[15] Roujean, J. L., Leroy, M., and Deschamps, P. Y., "A bidirectional reflectance model of the earth's surface for the correction of remote sensing data," *J. Geophys. Research* **97**(D18), 20455–20468 (1992).